

Article

Not peer-reviewed version

---

# Responsive Microgels Based on Raft-Hda Dynamic Covalent Bonding

---

Jingkai Nie , [Hang Yin](#) \* , Ruyue Cao , Changyuan Huang , Xiang Luo , Jun Ji

Posted Date: 21 December 2023

doi: 10.20944/preprints202312.1552.v1

Keywords: responsive microgels; hetero Diels-Alder (HDA) reactions; dynamic covalent bonding



Preprints.org is a free multidiscipline platform providing preprint service that is dedicated to making early versions of research outputs permanently available and citable. Preprints posted at Preprints.org appear in Web of Science, Crossref, Google Scholar, Scilit, Europe PMC.

Copyright: This is an open access article distributed under the Creative Commons Attribution License which permits unrestricted use, distribution, and reproduction in any medium, provided the original work is properly cited.

Article

# Responsive Microgels Based on RAFT-HDA Dynamic Covalent Bonding

Jingkai Nie <sup>1</sup>, Hang Yin <sup>1,\*</sup>, Ruyue Cao <sup>1</sup>, Changyuan Huang <sup>2</sup>, Xiang Luo <sup>2</sup> and Jun Ji <sup>1</sup>

<sup>1</sup> State Grid Smart Grid Research Institute Co. Ltd.; zhaoweimei@geiri.sgcc.com.cn

<sup>2</sup> China Electric Power Research Institute Co. Ltd.; shaoshuai@epri.sgcc.com.cn

\* Correspondence: yinhang@geiri.sgcc.com.cn; Tel.: +86 66601587

**Abstract:** In this paper, a method for the preparation of ultrasound-responsive microgels was developed based on RAFT-HDA dynamic covalent bonding. First, a styrenic cross-linked network was successfully prepared by DA reaction between phosphoryl dithioester and furan using double-ended BDEPDF as RAFT reagent mediated St polymerization as double-ended dienophile linker and copolymer of FMA and St as dienophile. Subsequently, the microgel system was constructed by the HDA reaction between phosphoryl disulfide and furan groups using the copolymer of polyethylene glycol monomethyl ether acrylate (OEGMA) and FMA as the dienophile building block and hydrophilic segment, and the polystyrene pro-dienophile linker as the cross-linker and hydrophobic segment. The number of furans in the dienophile chain and the length of the dienophile linker were regulated by RAFT polymerization to investigate the effects of single-molecule chain functional group degree (f), furan/dithioester ratio (r), and hydrophobic linker length (D) on the microgel system. These microgels can achieve the reversible transformation of materials under force responsiveness, and the steps are simple and adaptive, which are expected to show important potential applications in the fields of biomedical materials and adaptive electrical materials.

**Keywords:** responsive microgels, hetero Diels-Alder (HDA) reactions, dynamic covalent bonding

---

## 1. Introduction

The Diels-Alder (DA) reaction[1] is a well-known and commonly used organic cycloaddition reaction in chemical synthesis, materials science, and biomedicine[2-12]. The combinational pairing of dienes and dienophiles, which gives birth to a vast variety of DA reactions, is the central aspect of DA reactions. The inverse electron demand Diels-Alder reaction is a modern variation on traditional DA reactions like the reaction between furan and maleimide (iEDDA)[13]. The challenge with traditional DA reactions is their sluggish kinetics at room temperature, when equilibrium is either reached slowly or at very high temperatures. In order to achieve quantitative conversion, research has been done on effective Diels-Alder reactions such reversible addition fragmentation chain transfer-hetero Diels-Alder (RAFT-HDA) reactions, to reach quantitative conversion within minutes at ambient temperature[14].

Barnier-Kowollik proposed the RAFT-HDA reaction in 2008, based on the heteroatomic DA reaction between electron-absorbing dithioesters and cyclopentadiene or linear dienes. In general, an electron-absorbing dithioester acts as a chain transfer agent in reversible addition-break chain transfer (RAFT) polymerization to mediate monomer polymerization, followed by HDA reaction with corresponding dienes in the form of macromolecular chain end group as a dienophile. The RAFT-HDA reaction can be quantitatively converted in minutes to hours at room temperature or 50°C, allowing for the preparation of block polymers in water without the use of a catalyst. The RAFT-HDA reaction is beneficial for a variety of applications in high molecular weight block polymers (BCP), star-shaped polymers, surface modification, and biomedicine due to properties like high efficiency, speed, and reasonably good modularity[15-32]. The extensively researched RAFT-HDA reaction is based on a number of relatively electron-rich dithioesters, including diethoxyphosphoryl dithiocarbonate (BDEPDF) and benzyl pyridin-2-yl dithiocarbonate (BPDF), which act as dienophiles

and can effectively close the HOMO-LUMO gap in the DA reaction due to the electron-absorbing groups, leading to efficient and quick DA reactions. Cyclopentadienes and linear dienes make up the majority of all dienes. To obtain the building blocks with dienes as end groups for future reactions, the manufacture of dienes often needs several steps of reaction. Topological structures with higher complexity are characterized by more difficult steps and lower efficiency[33-36].

Microgels are characterized by a high water content, biocompatibility, and acceptable chemical and mechanical properties with changeable dimensions. They are functionalized nanoparticles with an internal three-dimensional cross-linked network. Applications in drug delivery, bioimaging, and other fields (coatings, catalysis, photonics) are made possible by the material's responsiveness to external stimuli (temperature, pH, light, electric field, and ionic strength)[37-43]. Microgels can be broadly divided into two kinds based on the molecular network structure: covalent cross-linking and supramolecular cross-linking. Free radical polymerization, click chemistry, Schiff base reaction, thiol-disulfide exchange reaction, and light reaction are the main covalent crosslinking techniques. Covalent cross-linking generally necessitates the introduction of various cross-linking agents into the microgel system in order to prepare precursors with various reactive functional groups. On the one hand, the introduction of cross-linking agents can result in the introduction of toxicity, but on the other hand, the preparation of microgels and the regulation of various properties necessitates more complex synthesis steps. Microgels formed by supramolecular cross-linking are based on the self-assembly polymerization of various physical interactions (including ionic, hydrophobic, and hydrogen bonds) and are typically prepared under mild conditions, primarily in water, to avoid toxic effects[44-51]. Gels formed by supramolecular cross-linking, on the other hand, may have lower mechanical strength and stability[52-57].Covalently cross-linked microgels are formed by coupling reactive functional groups, allowing for the modulation of the structure and properties of microgel particles with colloidal stability, which is required to prevent the gel network from dissociating and leaking drug. To prepare microgels with dynamic covalent bonding capable of maintaining strength while achieving functional flexibility, efforts to develop stable microgels with simple, efficient, and mild reaction conditions are critical.

Herein we achieved ultrasound responsive properties of the microgels as well as the release of model drug molecules using a simple preparation of responsive microgels based on RAFT-HDA dynamic covalent bonding. Firstly, the polymerization of styrene mediated by RAFT reagent with double-ended BDEPDF as a double-ended dienophile linker, and the copolymerization of furfuryl methacrylate (FMA) with styrene monomer to obtain a chain[58] pendant side group was used to realize the successful occurrence of DA reaction between phosphoryl disulfide and furan. Following that, the microgel system was created via HDA reaction between phosphoryl disulfide and furan groups, with the dienophile building block being a copolymer of poly(ethylene glycol monomethyl ether acrylate) (OEGMA) and FMA, and the cross-linker and hydrophobic segment being a polystyrene dienophile linker. We investigated the effects of single-molecule chain functional group degree (f), furan/dithioester ratio (r), and polystyrene linker length (D) on the DA reaction and thus on the microgel system by varying the number of furans in the dienophile chain and the length of the dienophile linker on the DA reaction and thus on the microgel system. We investigated the effects of single-molecule chain functional group degree (f), furan/dithioester ratio (r), and polystyrene linker length (D) on the DA reaction and consequently on the microgel system by varying the quantity of furans in the dienophile chain and the length of the dienophile linker because RAFT polymerization has good end-group retention and controllable molecular weight. These microgels have the ability to release model drug molecules under regulated conditions, and their mild, easy, and effective production processes are anticipated to have significant promise for use in areas like biomedical materials.

## 2. Materials and Methods

1,4-bis(bromomethyl)benzene (97%, Aladdin), sodium hydride (60% dispersion in mineral oil, Aladdin), tetrahydrofuran (THF) (anhydrous, ≥99.9%, J&K), diethyl phosphate (99.0%, Aladdin), carbon disulfide (anhydrous, ≥99.9%, Aladdin), toluene(Macklin), chloroform(J&K), dimethyl

sulfoxide (DMSO)(J&K), styrene(Amethyst,  $\geq 99.5\%$ ), silica gel(Aladdin), Polyethylene glycol monomethyl ether acrylate(OEGMA)(Mn=480, Aladdin,  $\geq 99\%$ ), Furfuryl methacrylate( $\geq 95\%$ , J&K), 2,2"-azobisisobutyronitrile (AIBN)( J&K), alkaline alumina(200-300 order, Macklin).The RAFT agents 1,4-phenylenebis(methylene)bis((diethoxyphosphoryl)methanedithioformate) (P-Di-linker) and 4-Cyano-4-(dodecyl trithiocarbonate)pentanoic acid(DDTCP)was prepared according to published procedures (Scheme S1, Supporting Information).

### Characterizations

$^1\text{H}$  Nuclear Magnetic Resonance (NMR) spectroscopy was performed on a AVANCE III 400 spectrometer operating at 400 MHz for hydrogen nuclei. All samples were dissolved in either  $\text{CDCl}_3$  or  $\text{DMSO}-d_6$ .

Gel permeation chromatography (GPC) system equipped with 10  $\mu\text{m}$  mixed columns in series and line with a 20 A refractive index detector (SEC) was used. The mobile phase of the instrument is  $N, N$ -dimethylacetamide (DMAC), the flow rate is  $1\text{ml}\cdot\text{min}^{-1}$ , the temperature of the gel chromatographic column rises to  $50^\circ\text{C}$ , and the standard curve is made by testing polystyrene with different molecular weights.

Light scattering (DLS) performed on a Malvern Zetasizer Nano series (Nano-ZS) instrument was used to measure the size of the microgels. The samples were illuminated with a 633 nm He–Ne laser, and the scattering light at a  $90^\circ$  angle was recorded using an avalanche photodiode detector.

Hitachi HT7700 transmission scanning electron microscope (TEM) was used to observe the morphology of micro gel with an observation voltage of 120 kV.

**Synthesis of Phosphoryl Disulfide Terminated Polystyrene(PS1-PS4).** Prepare a mixture of styrene monomer (in advance with alkaline alumina to remove the polymerization inhibitor), azo diisobutyronitrile (AIBN), and P-Di-linker in a Schlenk tube.

Oxygen and water were removed from the system through three freeze-evacuate-thaw cycles. The reaction was carried out at  $75^\circ\text{C}$  for 12 h, and then stopped by placing the solution in an ice water bath and exposing it to oxygen. The product mixture was precipitated three times by cold methanol and subsequently dried in a vacuum oven to obtain the corresponding products. The details of the four polymers are as follows ( PS1-[M]0/[RAFT]0/[AIBN]0=300:1:0.2, Mn=6689g. $\text{mol}^{-1}$ ,  $D=1.15$ , conversion=21%; PS2-[M]0/[RAFT]0/[AIBN]0=145:1:0.2, Mn=2832g. $\text{mol}^{-1}$ ,  $D=1.15$ , conversion=18.86%; PS3-[M]0/[RAFT]0/[AIBN]0=200:1:0.2, Mn=3987g. $\text{mol}^{-1}$ ,  $D=1.4$ , conversion=19.2%; PS4-[M]0/[RAFT]0/[AIBN]0=400:1:0.2, Mn=7563g. $\text{mol}^{-1}$ ,  $D=1.13$ , conversion=18.2% ) .

**Synthesis of Long Chain with Furan as Group vertical side group.** A mixture of styrene monomer or OEGMA, furfuryl methacrylate monomer (in advance with alkaline alumina to remove the inhibitor), azo diisobutyronitrile (AIBN), and DDTCP was prepared in a Schlenk tube. Oxygen and water were removed from the system by three freeze-evacuate-thaw cycles. The reaction was carried out at  $75^\circ\text{C}$  for 12h or 5h, and then stopped by placing the solution in an ice water bath and exposing it to oxygen. The copolymers of styrene and FMA were precipitated three times by cold methanol and the copolymers of OEGMA and FMA were precipitated three times by cold hexane, followed by drying in a vacuum oven to obtain the corresponding products. The details of several polymers are as follows ( SF1-[S]0/[F]0/[RAFT]0/[AIBN]0=150:44:1:0.2, conversiona=40%, conversionb=79.5%, [S]/[F]=60:35;SF2-[S]0/[F]0/[RAFT]0/[AIBN]0=115:20:1:0.2, conversiona=37.4%, conversionb=84.6%, [S]/[F]=43:17;OF1-[O]0/[F]0/[RAFT]0/[AIBN]0=55:5:1:0.2, conversiona=81.8%, conversionb=40%, [O]/[F]=45:2

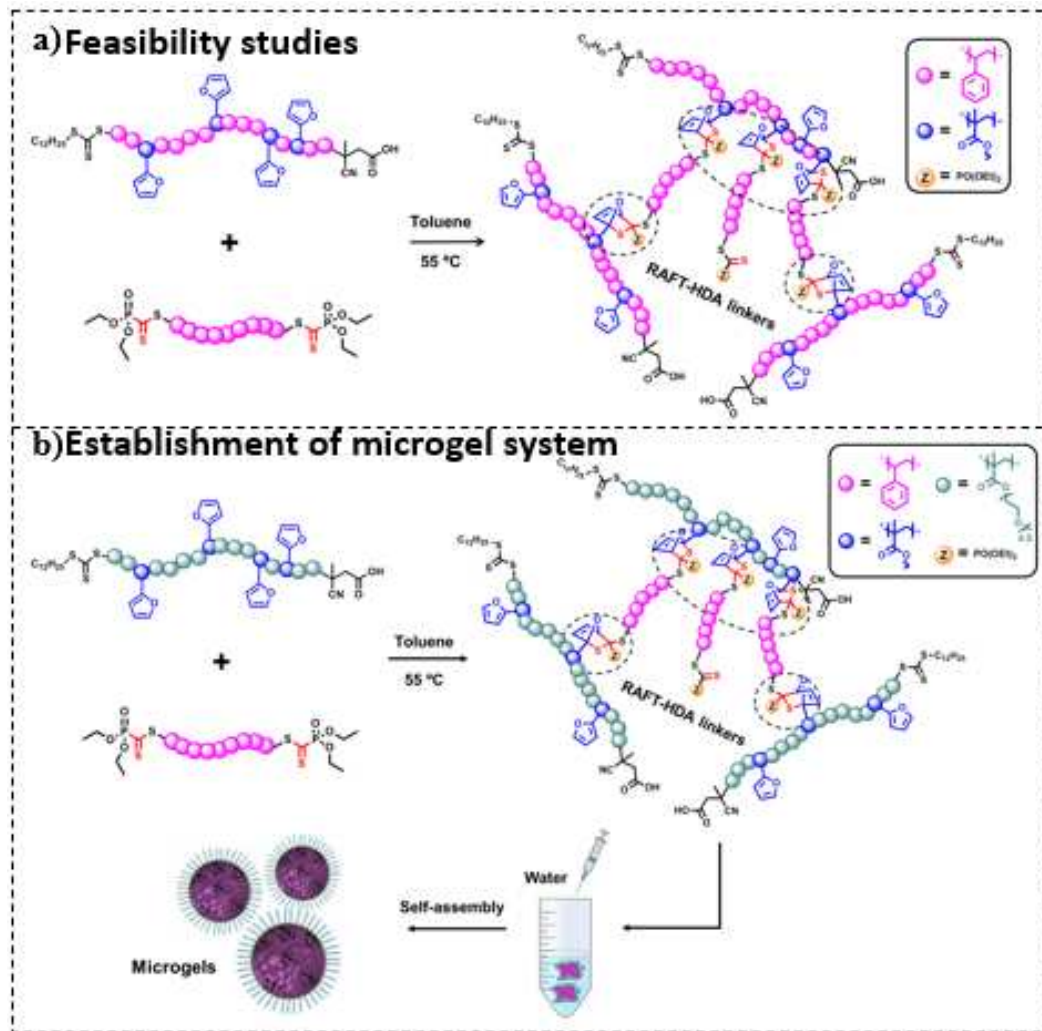
OF2-[O]0/[F]0/[RAFT]0/[AIBN]0=55:10:1:0.2, conversiona=81.8%, conversionb=40%, [O]/[F]=45:4;OF3-[O]0/[F]0/[RAFT]0/[AIBN]0=55:15:1:0.2, conversiona=81.8%, conversionb=46.7%, [O]/[F]=45:7;OF4-[O]0/[F]0/[RAFT]0/[AIBN]0=55:10:1:0.2, conversiona=72.7%, conversionb=50%, [O]/[F]=40:5.

**Reversible Addition Fragmentation Chain Transfer Hydro Diels–Alder Cyclization Between Phosphoryl Disulfides and Furan Rings.** The phosphoryl dithioester capped polymer and the pendant furan ring long chain polymer were dissolved in toluene, dissolve in a glass bottle with stirring and heat at  $55^\circ\text{C}$  for 24h. The resulting block copolymers were separated by precipitation in cold hexane and analyzed by GPC (THF or DMAC) and NMR ( $\text{CDCl}_3$ ).

**Preparation of Polymeric Microgels.** By pipetting 20 $\mu$ l of the reaction mixture with a pipette, add toluene and dilute to 0.6ml, then stir the diluted mixture for 10min. Ultra-pure water is then added dropwise to the mixture using a peristaltic pump at a rate of 0.67 mL.h<sup>-1</sup> until the desired volume ratio of water to toluene. The mixed solution is then placed in a cellulose dialysis strip and the toluene and unreacted building blocks are removed by ultra-pure water dialysis (water changes every 3 hours, at least 5 times). The solutions were subsequently used for TEM and DLS characterization.

### 3. Results and discussion

Scheme 1 depicts the main working concept. We prepared polystyrene with phosphoryl disulfide caps as the dienophile and a copolymer of FMA and styrene as the dienophile in order to test the viability of the HDA reaction between the phosphoryl disulfide and furan ring. By creating copolymers of FMA and OEGMA as in Scheme 1b, the concept of Scheme 1a was later expanded to include the creation of microgels. In the microgel system, polystyrene, a dienophile-type double-ended cross-linker, was subjected to an HDA reaction with OEGMA-co-FMA to produce microcrosslinked block polymers, in which polystyrene served as a hydrophobic segment and OEGMA as a hydrophilic segment. Following the HDA reaction, the hydrophilic balance of the system was then further assembled in aqueous solution to produce the microgel.



**Scheme 1.** (a) Construction of styrene-based network to verify reaction feasibility. (b) Construction of microgel system using RAFT-HDA reaction.

Polystyrene (PS1-PS4) was created by RAFT polymerization adopting 1,4-phenylbis(methylene) bis((diethoxyphosphoryl) methyl dithiocarbonate) as a chain transfer agent as the anticipated dienophile molecule in the HDA model concept (Scheme S2a). Simultaneously, 4-cyano-4-(dodecyl trithiocarbonate)pentanoic acid (DDTCP) was used to prepare RAFT copolymers of furfuryl methacrylate and styrene (SF1-SF2) (Scheme S2b) or Polyethylene glycol monomethyl ether acrylate (OF1-OF4) (Scheme S2c). Table 1 shows the molecular weight assessment of these building blocks.

**Table 1.** Summary of information on polymer samples.

Component	$f$	$M/f$ (g.mol <sup>-1</sup> ) <sup>1)</sup>	$M_n^a$	$M_n^b$	$D^b$	Blocks	$r$ ( $[F]_0/[S]_0$ ) <sup>1)</sup>	$[F]_0$ (mol.ML <sup>-1</sup> ) <sup>1)</sup>	$[S]_0$ (mol.ML <sup>-1</sup> ) <sup>1)</sup>	T (°C)	$M_n^b$	$D^b$
PSt1(S1)	2	3344	66	6689	6838	1.15						
PSt2(S2)	2	1416	28	2832	2765	1.15	OF4-S2	1	0.06	0.06	55	8696
PSt3(S3)	2	1993	39	3987	3767	1.4	OF4-S3	1	0.06	0.06	55	12586
PSt4(S4)	2	3781	75	7563	7209	1.13	OF4-S4	1	0.06	0.06	55	15428
P(St <sub>60</sub> -co-FMA <sub>35</sub> )(SF1)	35	351	95	10473	12289	1.19	SF1-S1	1	0.06	0.06	55	154080
P(St <sub>43</sub> -co-FMA <sub>17</sub> )(SF2)	17	443	60	7531	7483	1.15	SF2-S1	1	0.06	0.06	55	213879
P(OEGMA <sub>45</sub> -co-FMA <sub>2</sub> )(OF1)	2	2566	47	5133	4743	1.54	OF1-S3	1	0.06	0.06	55	10434
P(OEGMA <sub>45</sub> -co-FMA <sub>4</sub> )(OF2)	4	1375	49	5501	5498	1.26	OF2-S3	1	0.06	0.06	55	19380
P(OEGMA <sub>45</sub> -co-FMA <sub>7</sub> )(OF3)	7	860	52	6021	7902	1.03	OF3-S3	1	0.06	0.06	55	3162
OF4-S2												
P(OEGMA <sub>40</sub> -co-FMA <sub>5</sub> )(OF4)	5	952	42	4763	4477	1.38	OF4-S3	2	0.12	0.06	55	gel
OF4-S4												

The produced polymers were evaluated by <sup>1</sup>H NMR analysis to ascertain the structure of the aforementioned polymers. All of the distinctive peaks of the RAFT reagent, dienophile, and pro-dienophile building blocks can be seen in Figure 1. As seen in Figure 1a, the characteristic peaks in proton signals b,d corresponding to phosphoryl disulfide show that the P-Di-linker successfully mediated the polymerization of styrene, resulting in the presence of a well-defined disulfide end group. In addition, the characteristic peaks in proton signals A,a,C,D,c,d corresponding to styrene, ethylene glycol, and furan. In order to investigate the feasibility of the reaction of phosphoryl dithioesters with furan HDA, two sets of dienophile building blocks of different lengths and different numbers of furan units, SF1 an characterized by several different means.

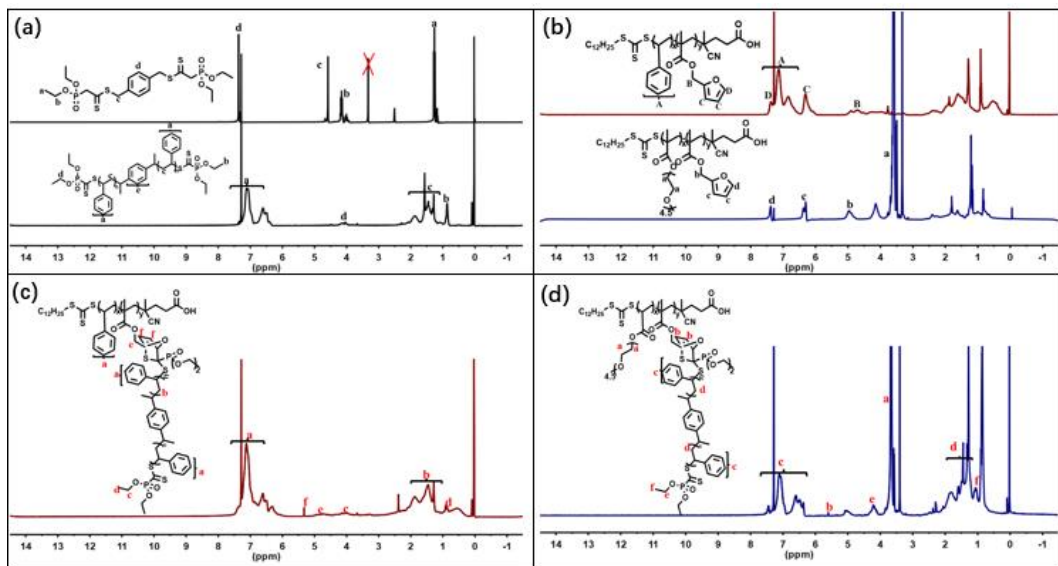


**Figure 1.**  $^1\text{H}$  NMR spectra of the typical synthetic products.

In the  $^1\text{H}$  NMR analysis (Figure 1c), the proton signals f correspond to the formation of new double-bonded hydrogen characteristic peaks after the cycloaddition reaction of the furan ring with the dithioester ring. Figure 2a,b then gives the relationship between the molecular weights of the two sets of reaction building blocks and the block copolymers. The GPC chromatograms show the traces of the formed block copolymers relative to the individual building blocks. The significantly reduced retention time of the traces and the absence of significant shoulders also indicate successful and effective block formation, which is consistent with the data in Table 1. It should be emphasized that none of the block copolymers produced in the current investigation were pure when they underwent GPC testing. We can infer from the GPC spectra of the block copolymers that the grafting rate of the block system, or the effectiveness of the HDA reaction, is influenced by the length of the block and the number of furan units in a single diene building block. This, in turn, results in a variety of molecular weights and molecular weight distributions for the system. This item was not thoroughly explored, and the microgel part will be investigated at and confirmed.

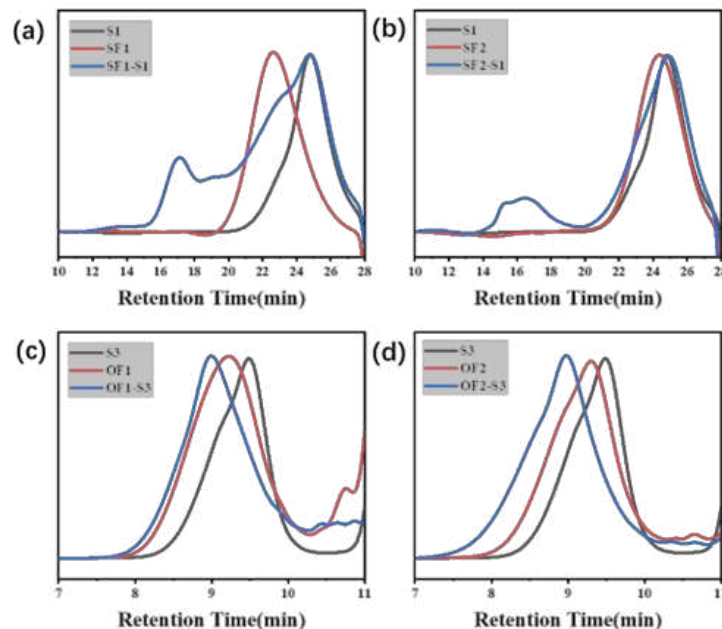


**Figure 2.** (a), (b) Comparison of molecular weight before and after reaction of styrene-based network HDA. (c), (d) Comparison of molecular weight before and after HDA reaction of microgel system.

To further examine the thermal reversibility of the Diels-Alder reaction in the system, DSC and variable temperature FTIR were applied. It is possible to visualize the system after the HDA reaction in the DSC curve with a heat absorption peak at approximately 120°C (Figure 3b), which corresponds to the inverse DA reaction of the DA bond between the furan and dithioester and also supports the viability of the HDA reaction between the furan ring and phosphoryl dithioester from the side. The cross-linked polymers were analyzed by variable temperature FTIR spectroscopy in addition to DSC (Fig. 3a). The technique is highly sensitive to the exact molecular structures created by the Diels-Alder and reverse Diels-Alder processes being absorbed. The samples were heated to a temperature over the 120 °C threshold for the inverse DA reaction, a gradient of 20 °C was set, and each temperature was kept for 10 minutes before the corresponding analysis, which consisted of heating and cooling for one cycle, was conducted. With symmetric and asymmetric stretching vibrations of the intra-ring C- O- C bonds, furan rings have the cyclic bis(vinyl ether) structure that is typical of these compounds. Asymmetric stretching vibrations of the ring's C- O- C bonds occur in furan acrylates at a frequency of 1220 cm<sup>-1</sup>. The cyclic C-O-C bond's asymmetric stretching vibration occurs at a frequency of 1220 cm<sup>-1</sup> in -furan acrylate, while its symmetric stretching vibration occurs at a reasonably steady frequency of 1076 cm<sup>-1</sup> and is less affected by the substituent. [IR analysis of the structure and IR spectral features of  $\alpha$ -furan esters]. The characteristic peaks at 1030 cm<sup>-1</sup> and in the range of 1750–2400 cm<sup>-1</sup> vary in the spectra of the cross-linked polymers. The analysis shows that the stretching vibration of the C-O-C bond, which is responsible for the absorption band at 1030 cm<sup>-1</sup>, the stretching vibration of the carbonyl group, which is responsible for the absorption band at 1750 cm<sup>-1</sup>, and the variation of the absorption intensity of the C=C=O bond, which is responsible for the absorption band at 2400-2150 cm<sup>-1</sup>. As can be seen, as the temperature rises, the system experiences an inverse DA reaction and the relevant IR characteristic peaks' absorption intensities vary accordingly. However, the system's recyclability is relatively poor. However, the feasibility of the HDA reaction in this system can be confirmed, and Figure S1 further shows that the system is reversible. The pro-dienophile building block PS, dienophile building block SF, and SF-S block polymerization's typical TGA curves are shown in Figure 3c. As can be observed, the inclusion of FMA lowers the temperature at which breakdown begins but raises the quantity of carbon that is still present at 700°C. A greater amount of residual char was left after the crosslinking with PS, which is more proof that the crosslinking was successful. The degree of crosslinking and the amount of residual char are directly connected, and the relative amount of FMA is proportional to both (Figure S2). It is important to note that the stability of the system decreased after the reaction, which can be attributed to the further increase in the amount of FMA after the grafting of the system, the fact that the cross-linked system did not form a large cross-link density, the fact that the reaction system was not purified and there were unreacted building blocks.

As a result of the research above, we expand the DA reaction between furan and phosphoryl disulfide to create a microgel system. The amount of functional groups (f) of single-chain polystyrene is fixed at 2, and the disulfide ester and furan ring exist here as cross-linking reaction sites. The number of furan sites of single-chain furan copolymer can be adjusted, but it is not advisable to have too many as cross-linking reaction sites for the creation of microgel system. At the same time, OEGMA and polystyrene interact to generate hydrophilic linkage segments and comb, trapezoidal, or smaller cross-link density block polymers, depending on the molecular structure of the copolymer. Here, we used adjustable RAFT polymerization to create microgels more easily while examining the impact of hydrophobic segment length and cross-link density on the microgel system.

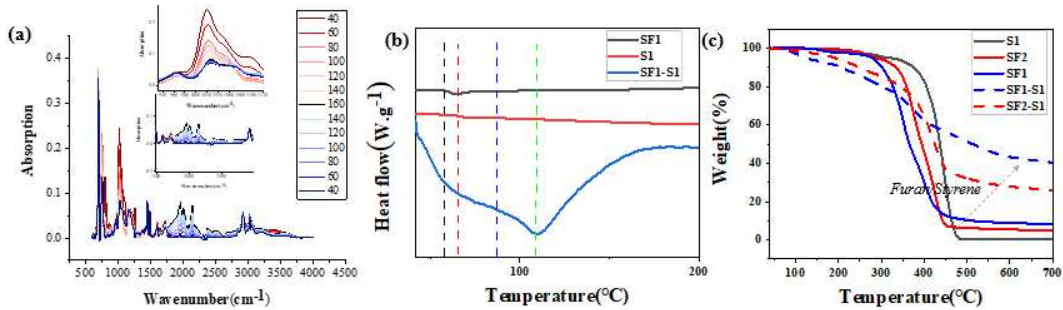


**Figure 3.** (a) Variable temperature FTIR spectroscopy in addition to DSC of cross-linked polymers. (b) DSC curve of the system after the HDA reaction. (c) TGA curves of pro-dienophile building block PS, dienophile building block SF, and SF-S block polymerization.

We first prepared polystyrene of three different lengths (DP 30, 40, and 80, respectively) of S2, S3, and S4 as crosslinkers in order to investigate the impact of hydrophobic chain segment length on microgels. We then obtained a series of solutions containing the S/OF reaction system by controlling the dithioester to furan ratio of 1 ( $r=1$ ), reacting with OF4 via HDA, and performing subsequent microgel preparation (for details, see Experimental section). The size and shape of the grafted polymer aggregates were investigated using transmission electron microscopy (TEM). The TEM morphology supported our prior theory that the polymers generated from the S/OF process were capable of forming microgel structures in water, as illustrated in Figure S3. Meanwhile, the TEM images and DLS data show (Figure 4) that the size of the microgel gradually increases with the length of the hydrophobic segment. This is explained by the fact that as the hydrophobic part of the system grows, the system must reach a new affinity for water, which results in a corresponding change in the microgel size. The crosslinking density of the microgel system, which has varied impacts on the particle size and dispersion of the microgel, is affected by the size of the building block for the DA reaction as well.

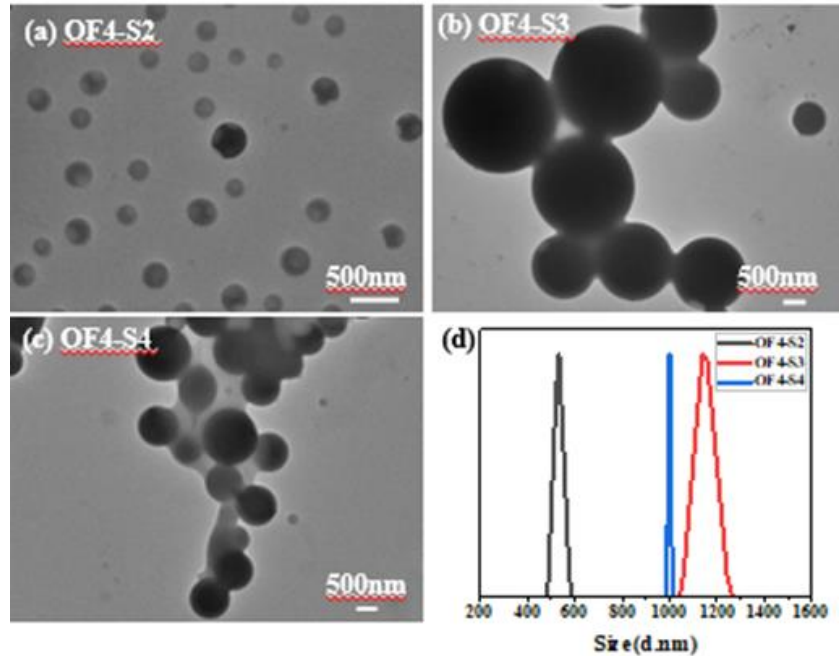


**Figure 4.** (a), (b), (c) TEM images of microgel systems with different lengths of hydrophobic segments. (d) DLS images of microgel systems with different lengths of hydrophobic segments.

The control group (Figure 5) with varying water concentrations (40–80v%) demonstrates, that the water content has no effect on the microgels' fundamental spherical form. We explain this by the formation of a micro-crosslinked network structure that is difficult to change, which is coupled by

DA bonds between the hydrophobic chain segment S and the hydrophilic chain segment OF. According to the TEM images, however, the existence of numerous stiff benzene rings on the molecular weight also contributes to the production of a few components, such as bowl-shaped morphology and porous morphology, because the hydrophobic chain segment of the system is polystyrene. Naturally, this has some research value as well and won't be covered here. The DLS data show that the microgel's particle size fluctuates with increasing water content but does not change appreciably either way.

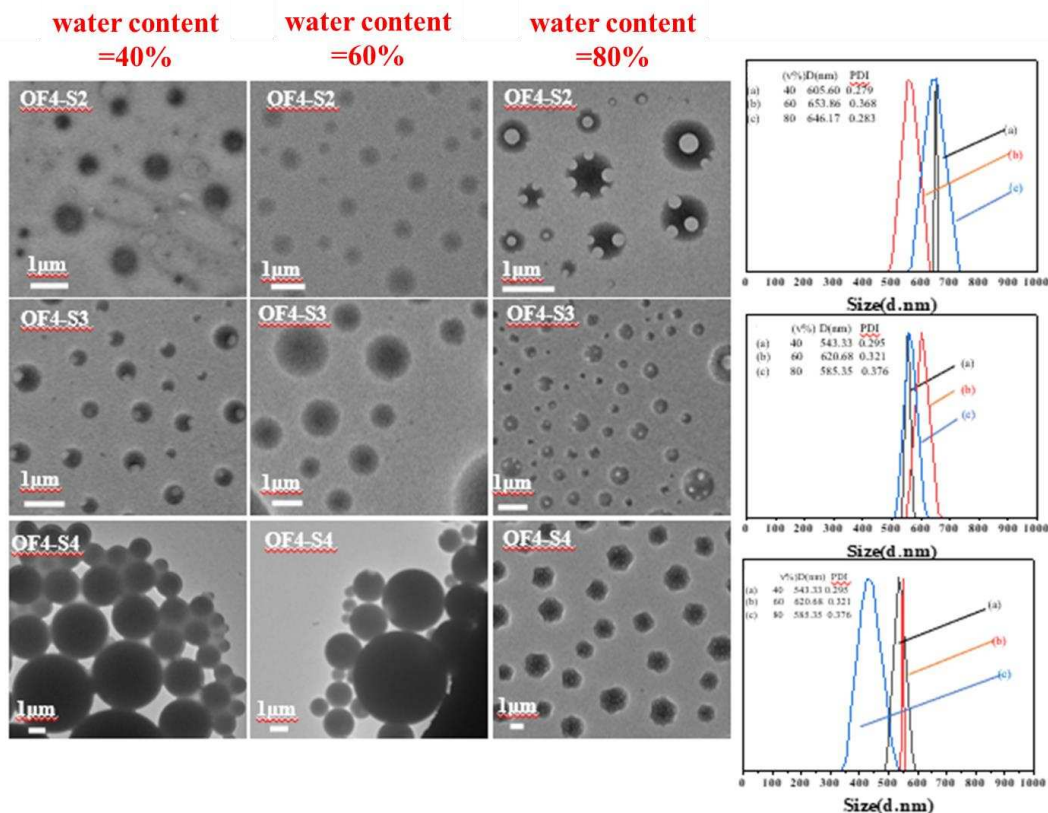


**Figure 5.** Effect of water content on the morphology and particle size of microgels with different lengths of hydrophobic segments.

In subsequent experiments, we simply and effectively controlled the number of cross-linking sites by regulating the number of furan groups in single chains via RAFT polymerization regulation, achieving the goal of controlling the cross-linking density of the cross-linked system. To investigate the effect of crosslinking density on the microgel system, we prepared OEGMA-co-FMA block copolymers OF1, OF2, OF3 (=2, 4, 7) containing varying numbers of furan units while keeping the length of hydrophobic and hydrophilic chains constant. The morphology of the resulting microgels composed of S3 and OF with different is shown in TEM images after a similar preparation process (Figure 6). The microgels of various crosslinking densities have a spherical shape. As the number of single-chain furan units rises, the system's crosslinking density also rises along with it, as does the number of linked hydrophobic chain segments. This results in a general increase in gel size as well as a corresponding narrowing of the particle size distribution. It should be noted that the research of the hydrophobic chain length and the amount of single-chain furan units both rely on the same initial functional group concentration and a dithioester/furan ratio of 1 ( $[S]/[F] = r = 1$ ). Next, we investigate how  $r$  affects the microgel system. Using  $r=2$  for the corresponding reaction process, we find that too much furan causes the system to gel, resulting in an insoluble fraction. Only a small amount of soluble fraction is needed for the corresponding characterization, which reveals that the large aggregated system is not a properly prepared microgel (Figure S4). The microgels made using this method also exhibit good stability; just a small amount of precipitation was discovered in the system after 36 days

in a normal environment, and the solution of the microgel system changed from pure white to translucent white. The accumulation is more significant.

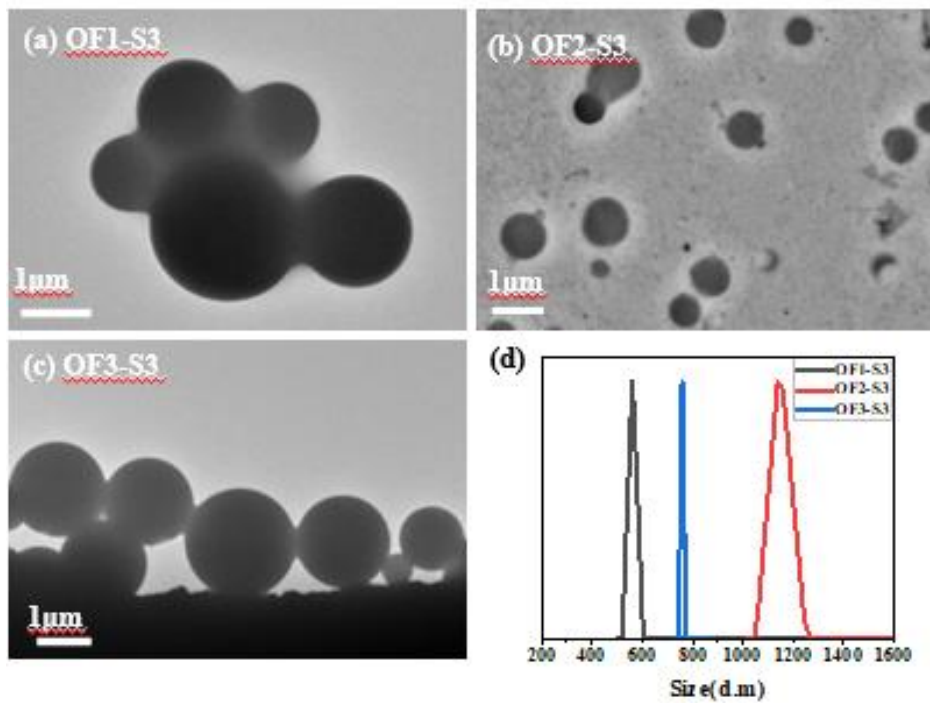


**Figure 6.** (a), (b), (c) TEM images of microgels with different diene cell numbers. d) DLS images of microgel systems with different diene cell numbers.

Microgels have the potential for biomedical applications such as controlled release because of their response to external stimuli. At the moment, temperature and pH variations are the main focus of microgels' responsiveness. The microgel system's responsiveness to temperature is often constrained by the type of polymer used and depends on its LCST properties. The manufacture of microgels with physically cross-linked structures necessitates the use of unique molecules and structures, which is a dilemma because the reaction to pH typically depends on specific bonding, such as hydrogen bonding.

The DA bond created by the RAFT-HDA reaction is thermally reversible, but still up to a temperature of 120 °C, according to the study mentioned above. Despite the fact that the DA bond will break to give the microgel a stimulating responsiveness, the microgel at this temperature will undoubtedly disintegrate owing to the high temperature and will not match the application requirements of microgel. In 2014, Zhijian Wang's team created a brand-new mechanical carrier made of At room temperature, this polymer can undergo an inverse HDA reaction through ultrasonication, which will cause the system to disintegrate and give it force-responsive characteristics. Inspiring by the aforementioned, we undertook a cursory research of the force responsiveness of the HDA bond between the furan ring and phosphoryl dithioester. We chose two systems, OF3-S2 and OF4-S2, for 2 hours of sonication to test the microgel systems' force responsiveness. Figures 7a,b show the phenomena of polystyrene molecules separating from the microgels and generating flocculent precipitates. Gel chromatography analysis will reveal that the molecular weight of the sonicated systems significantly decreased, and lower peaks appeared in the higher molecular weight fraction corresponding to the non-detached fraction (Figure 7c,d). The analysis was subsequently expanded upon by coating rhodamine B.

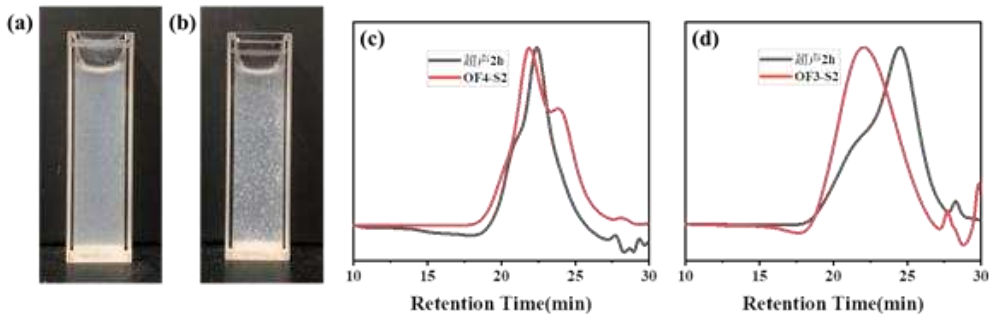


**Figure 7.** (a) , (b) Macroscopic behavior of microgel assemblies in water before and after ultrasound. c , d) Molecular weight changes before and after 2h sonication for different microgel systems.

Rhodamine B was coated by the microgel technique at a comparatively high rate, as seen in Figure 8. The bonding of the microgel system was broken after sonication, which therefore reduced the pace at which the medication was coated. The particle size change of the microgel particles was also noticeably smaller after sonication. The mechanical force that disrupts the bonding between the polystyrene and copolymer chain segments, which results in the microgel system's disruption and gives the microgel force responsiveness, is thought to be responsible for the results mentioned above. However, further research must be done to determine the precise mechanism and contributing elements.

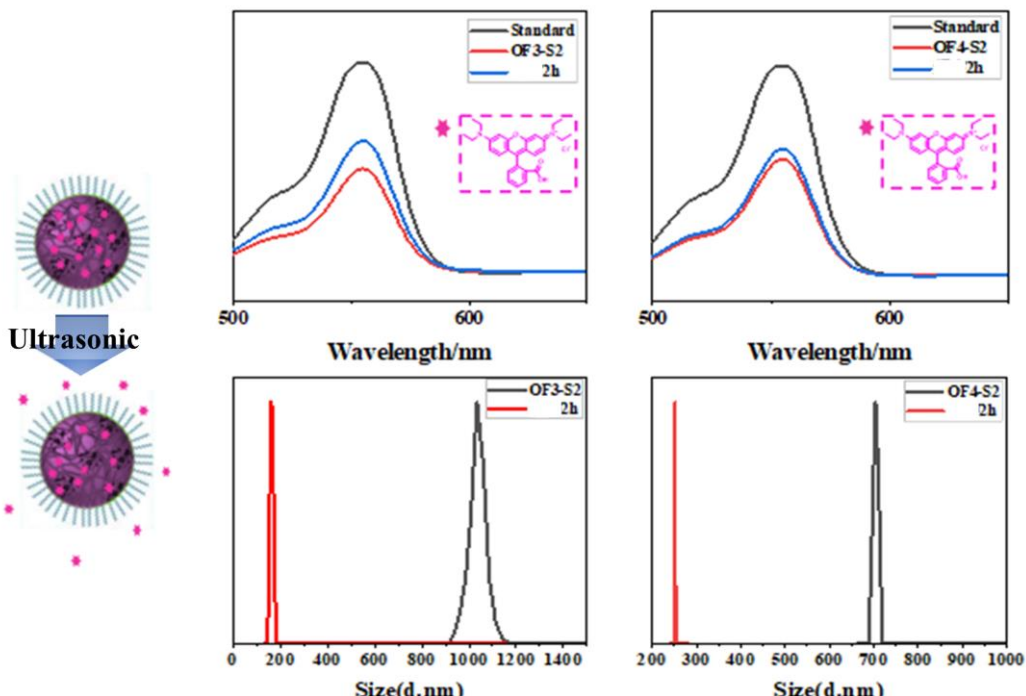


**Figure 8.** Changes in drug loading and particle size of different microgel systems before and after 2h sonication.

#### 4. Conclusions

In conclusion, Finally, based on the cascade reaction of RAFT polymerization and Diels-Alder, this paper investigates a new diene, furan ring, for the HDA reaction, and applies the new RAFT-HDA reaction to the preparation of microgels. On the one hand, the furan ring can participate in the HDA reaction, providing a more readily available dienophile for the RAFT-HDA reaction, expanding the variety of dienophiles in the RAFT-HDA reaction system, and making it easier to obtain more complex topologies from RAFT-HDA; on the other hand, the RAFT-HDA reaction can be extended to some extent for more applications. In this paper, we investigate the effects of

hydrophobic chain length and crosslinking density on microgel systems, and we obtain stable microgel assemblies in a very simple way, while achieving easy modulation of their properties thanks to the introduction of controllable RAFT polymerization, which makes them mechanically responsive. The presence of furan rings in a very large number of monomers and their investigation as novel dienes gives more possibilities for the RAFT-HDA reaction. In this paper, we investigate the effects of hydrophobic chain length and crosslinking density on microgel systems, and we obtain stable microgel assemblies in a very straightforward manner while achieving easy property modulation thanks to the introduction of controllable RAFT polymerization. Furan rings are found in a very large number of monomers, and their research as novel dienes expands the RAFT-HDA reaction's potential.

**Supplementary Materials:** Visible in the Support Information.

**Author Contributions:** Conceptualization, Jingkai Nie; methodology, Hang Yin; Validation, Ruyue Cao and Hang Yin; feasibility analysis, Changyuan Huang and Xiang Luo; data curation, Jun Ji; writing—original draft preparation, Hang Yin; project administration, Jingkai Nie; funding acquisition, Changyuan Huang and Xiang Luo. All authors have read and agreed to the published version of the manuscript.

**Funding:** This research was funded by Technical research service project "Research support for structural toughness improvement and carbon reduction technology evaluation of power transmission and transformation", State Grid Corporation of China, project number SGZB0000JJJS2300402.

**Institutional Review Board Statement:** "Not applicable" for studies not involving humans or animals.

**Data Availability Statement:** There is no other data were created during this study.

**Acknowledgments:** Acknowledge to the colleagues and collaborators who supported the research and the institutions and individuals that provided equipment support.

**Conflicts of Interest:** The authors declare no conflict of interest.

## References

1. Chiehari J, Chong Y K, Ercole F, et al. Living Free-Radical Polymerization by Reversible Addition-Fragmentation Chain Transfer: The Raft Process [J]. *Macromolecules*, 1998, 31(16): 5559-5562.
2. Moad G, Rizzardo E, Thang S H. Living Radical Polymerization by the Raft Process – a Third Update [J]. *Australian Journal of Chemistry*, 2012, 65.
3. Hu W, Ren Z, Li J, et al. New Dielectric Elastomers with Variable Moduli [J]. *Advanced Functional Materials*, 2015, 25(30): 4827-4836.
4. Molev G, Lu Y, Kim K S, et al. Organometallic-Polypeptide Diblock Copolymers: Synthesis by Diels–Alder Coupling and Crystallization-Driven Self-Assembly to Uniform Truncated Elliptical Lamellae [J]. *Macromolecules*, 2014, 47(8): 2604-2615.
5. Chang H, Kim M S, Huber G W, et al. Design of Closed-Loop Recycling Production of a Diels-Alder Polymer from a Biomass-Derived Difuran as a Functional Additive for Polyurethanes [J]. *Green Chem*, 2021, 23(23): 9479-9488.
6. Bowman C, Du Prez F, Kalow J. Introduction to Chemistry for Covalent Adaptable Networks [J]. *Polymer Chemistry*, 2020, 11(33): 5295-5296.
7. Xu X, Ma S, Wang S, et al. Fast-Reprocessing, Postadjustable, Self-Healing Covalent Adaptable Networks with Schiff Base and Diels-Alder Adduct [J]. *Macromol Rapid Commun*, 2022, 43(13): e2100777.
8. Rinehart J M, Reynolds J R, Yee S K. Limitations of Diels–Alder Dynamic Covalent Networks as Thermal Conductivity Switches [J]. *ACS Applied Polymer Materials*, 2022, 4(2): 1218-1224.
9. Li X, Yu R, He Y, et al. Four-Dimensional Printing of Shape Memory Polyurethanes with High Strength and Recyclability Based on Diels-Alder Chemistry [J]. *Polymer*, 2020, 200.
10. Hirschbiel A F, Konrad W, Schulze-Sunninghausen D, et al. Access to Multiblock Copolymers Via Supramolecular Host-Guest Chemistry and Photochemical Ligation [J]. *ACS Macro Lett*, 2015, 4(10): 1062-1066.
11. Hu Y, Zhang J, Miao Y, et al. Enzyme-Mediated in Situ Self-Assembly Promotes in Vivo Bioorthogonal Reaction for Pretargeted Multimodality Imaging [J]. *Angew Chem Int Ed Engl*, 2021, 60(33): 18082-18093.
12. Masson G, Lalli C, Benohoud M, et al. Catalytic Enantioselective [4 + 2]-Cycloaddition: A Strategy to Access Aza-Hexacycles [J]. *Chem Soc Rev*, 2013, 42(3): 902-923.
13. Knall A C, Slugovc C. Inverse Electron Demand Diels-Alder (Iedda)-Initiated Conjugation: A (High) Potential Click Chemistry Scheme [J]. *Chem Soc Rev*, 2013, 42(12): 5131-5142.

14. Geng Z, Shin J J, Xi Y, et al. Click Chemistry Strategies for the Accelerated Synthesis of Functional Macromolecules [J]. *Journal of Polymer Science*, 2021, 59(11): 963-1042.
15. Espinosa E, Glassner M, Boisson C, et al. Synthesis of Cyclopentadienyl Capped Polyethylene and Subsequent Block Copolymer Formation Via Hetero Diels-Alder (Hda) Chemistry [J]. *Macromolecular Rapid Communications*, 2011, 32(18): 1447-1453.
16. Nebhani L, Schmiedl D, Barner L, et al. Quantification of Grafting Densities Achieved Via Modular 'Grafting-to' Approaches onto Divinylbenzene Microspheres [J]. *Advanced Functional Materials*, 2010, 20(12): P.2010-2020.
17. Tischer T, Goldmann A S, Linkert K, et al. Modular Ligation of Thioamide Functional Peptides onto Solid Cellulose Substrates [J]. *Advanced Functional Materials*, 2012, 22(18): 3853-3864.
18. Kaupp M, Vogt A P, Natterrot J C, et al. Modular Design of Glyco-Microspheres Via Mild Pericyclic Reactions and Their Quantitative Analysis [J]. *Polymer Chemistry*, 2012, 3(9): 2605-2614.
19. Inglis A J, Sinnwell S, Davis T P, et al. Reversible Addition Fragmentation Chain Transfer (Raft) and Hetero-Diels?Alder Chemistry as a Convenient Conjugation Tool for Access to Complex Macromolecular Designs [J]. *MACROMOLECULES*, 2008, 41(12): 4120-4126.
20. Sinnwell S, Inglis A J, Davis T P, et al. An Atom-Efficient Conjugation Approach to Well-Defined Block Copolymers Using Raft Chemistry and Hetero Diels?Alder Cycloaddition [J]. *Chemical Communications*, 2008, 19(17): 2052-2054.
21. Sinnwell S, Inglis A J, Stenzel M H, et al. Access to Three-Arm Star Block Copolymers by a Consecutive Combination of the Copper(I)-Catalyzed Azide?Alkyne Cycloaddition and the Raft Hetero Diels?Alder Concept [J]. *Macromolecular Rapid Communications*, 2008, 29(12-13).
22. Bousquet A, Barner-Kowollik C, Stenzel M H. Synthesis of Comb Polymers Via Grafting-onto Macromolecules Bearing Pendant Diene Groups Via the Hetero-Diels-Alder-Raft Click Concept [J]. *Journal of Polymer Science Part A Polymer Chemistry*, 2010, 48(8): 1773-1781.
23. Sebastian, Sinnwell, Mieke, et al. Efficient Access to Multi-Arm Star Block Copolymers by a Combination of Atrp and Raft-Hdaclickchemistry [J]. *Journal of Polymer Science Part A: Polymer Chemistry*, 2009.
24. Beloqui A, Mane S R, Langer M, et al. Hetero-Diels?Alder Cycloaddition with Raft Polymers as Bioconjugation Platform [J]. *Angewandte Chemie International Edition*, 2020.
25. Inglis A J, Paulöhr T, Barner-Kowollik C. Ambient Temperature Synthesis of a Versatile Macromolecular Building Block: Cyclopentadienyl-Capped Polymers [J]. *Macromolecules*, 2009, 43(1): 33-36.
26. Inglis A J, Stenzel M H, Barner-Kowollik C. Ultra-Fast Raft-Hda Click Conjugation: An Efficient Route to High Molecular Weight Block Copolymers [J]. *Macromol Rapid Commun*, 2009, 30(21): 1792-1798.
27. Langer M, Brandt J, Lederer A, et al. Amphiphilic Block Copolymers Featuring a Reversible Hetero Diels-Alder Linkage [J]. *Polym Chem*, 2014, 5(18): 5330-5338.
28. Dürr C J, Hlalele L, Kaiser A, et al. Mild and Efficient Modular Synthesis of Poly(Acrylonitrile-Co-Butadiene) Block and Miktoarm Star Copolymer Architectures [J]. *Macromolecules*, 2012, 46(1): 49-62.
29. Zydziak N, Hübner C, Bruns M, et al. One-Step Functionalization of Single-Walled Carbon Nanotubes (Swcnts) with Cyclopentadienyl-Capped Macromolecules Via Diels?Alder Chemistry [J]. *Macromolecules*, 2011, 44(9): 3374-3380.
30. Zydziak N, Preuss C M, Winkler V, et al. Hetero Diels-Alder Chemistry for the Functionalization of Single-Walled Carbon Nanotubes with Cyclopentadienyl End-Capped Polymer Strands [J]. *Macromol Rapid Commun*, 2013, 34(8): 672-680.
31. Guimard N K, Ho J, Brandt J, et al. Harnessing Entropy to Direct the Bonding/Debonding of Polymer Systems Based on Reversible Chemistry [J]. *Chemical Science*, 2013, 4(7).
32. Schenzel A M, Klein C, Rist K, et al. Reversing Adhesion: A Triggered Release Self-Reporting Adhesive [J]. *Advanced Science*, 2016, 3(3): 1500361.
33. Glassner M, Kempe K, Schubert U S, et al. One-Pot Synthesis of Cyclopentadienyl Endcapped Poly(2-Ethyl-2-Oxazoline) and Subsequent Ambient Temperature Diels-Alder Conjugations [J]. *Chem Commun (Camb)*, 2011, 47(38): 10620-10622.
34. Brandt J, Lenz J, Pahnke K, et al. Investigation of Thermoreversible Polymer Networks by Temperature Dependent Size Exclusion Chromatography [J]. *Polymer Chemistry*, 2017, 8(43): 6598-6605.
35. Oehlenschlaeger K K, Mueller J O, Brandt J, et al. Adaptable Hetero Diels-Alder Networks for Fast Self-Healing under Mild Conditions [J]. *Adv Mater*, 2014, 26(21): 3561-3566.
36. Mutlu H, Schmitt C W, Wedler-Jasinski N, et al. Spin Fluorescence Silencing Enables an Efficient Thermally Driven Self-Reporting Polymer Release System [J]. *Polymer Chemistry*, 2017, 8(40): 6199-6203.
37. Oh J K, Drumright R, Siegwart D J, et al. The Development of Microgels/Nanogels for Drug Delivery Applications [J]. *Progress in Polymer Science*, 2008, 33(4): 448-477.
38. Oh J K, Lee D I, Park J M. Biopolymer-Based Microgels/Nanogels for Drug Delivery Applications [J]. *Progress in Polymer Science*, 2009, 34(12): 1261-1282.

39. Wiemer K, Dormbach K, Slabu I, et al. Hydrophobic Superparamagnetic Fept Nanoparticles in Hydrophilic Poly(N-Vinylcaprolactam) Microgels: A New Multifunctional Hybrid System [J]. *J Mater Chem B*, 2017, 5(6): 1284-1292.

40. Karg M. Multifunctional Inorganic/Organic Hybrid Microgels [J]. *Colloid and Polymer Science*, 2012, 290(8): 673-688.

41. Peng L, Feng A, Liu S, et al. Electrochemical Stimulated Pickering Emulsion for Recycling of Enzyme in Biocatalysis [J]. *ACS Appl Mater Interfaces*, 2016, 8(43): 29203-29207.

42. Zhang H, Niu C, Zhang Y, et al. A Mechanically Strong Polyvinyl Alcohol/Poly(2-(N,N'-Dimethyl Amino) Ethyl Methacrylate)-Poly (Acrylic Acid) Hydrogel with Ph-Responsiveness [J]. *Colloid and Polymer Science*, 2020, 298(6): 619-628.

43. Sasaki Y, Akiyoshi K. Nanogel Engineering for New Nanobiomaterials: From Chaperoning Engineering to Biomedical Applications [J]. *Chem Rec*, 2010, 10(6): 366-376.

44. Rossow T, Heyman J A, Ehrlicher A J, et al. Controlled Synthesis of Cell-Laden Microgels by Radical-Free Gelation in Droplet Microfluidics [J]. *J Am Chem Soc*, 2012, 134(10): 4983-4989.

45. Li B, Jiang X, Yin J. Multi-Responsive Microgel of Hyperbranched Poly(Ether Amine) (Hpea-Mgel) for the Selective Adsorption and Separation of Hydrophilic Fluorescein Dyes [J]. *Journal of Materials Chemistry*, 2012, 22(34).

46. Steinhilber D, Rossow T, Wedepohl S, et al. A Microgel Construction Kit for Bioorthogonal Encapsulation and Ph-Controlled Release of Living Cells [J]. *Angew Chem Int Ed Engl*, 2013, 52(51): 13538-13543.

47. Bahadur K C R, Xu P. Multicompartment Intracellular Self-Expanding Nanogel for Targeted Delivery of Drug Cocktail [J]. *Adv Mater*, 2012, 24(48): 6479-6483.

48. Zhang J, Yang F, Shen H, et al. Controlled Formation of Microgels/Nanogels from a Disulfide-Linked Core/Shell Hyperbranched Polymer [J]. *ACS Macro Lett*, 2012, 1(11): 1295-1299.

49. Yan L, Tao W. One-Step Synthesis of Pegylated Cationic Nanogels of Poly(N,N'-Dimethylaminoethyl Methacrylate) in Aqueous Solution Via Self-Stabilizing Micelles Using an Amphiphilic Macroraft Agent [J]. *Polymer*, 2010, 51(10): 2161-2167.

50. Heller D A, Levi Y, Pelet J M, et al. Modular 'Click-in-Emulsion' Bone-Targeted Nanogels [J]. *Adv Mater*, 2013, 25(10): 1449-1454.

51. Tan H, Jin H, Mei H, et al. Peg-Urokinase Nanogels with Enhanced Stability and Controllable Bioactivity [J]. *Soft Matter*, 2012, 8(9).

52. Kim K, Bae B, Kang Y J, et al. Natural Polypeptide-Based Supramolecular Nanogels for Stable Noncovalent Encapsulation [J]. *Biomacromolecules*, 2013, 14(10): 3515-3522.

53. Nakai T, Hirakura T, Sakurai Y, et al. Injectable Hydrogel for Sustained Protein Release by Salt-Induced Association of Hyaluronic Acid Nanogel [J]. *Macromol Biosci*, 2012, 12(4): 475-483.

54. Hasegawa U, Sawada S, Shimizu T, et al. Raspberry-Like Assembly of Cross-Linked Nanogels for Protein Delivery [J]. *J Control Release*, 2009, 140(3): 312-317.

55. Hirakura T, Yasugi K, Nemoto T, et al. Hybrid Hyaluronan Hydrogel Encapsulating Nanogel as a Protein Nanocarrier: New System for Sustained Delivery of Protein with a Chaperone-Like Function [J]. *J Control Release*, 2010, 142(3): 483-489.

56. Sasaki Y, Asayama W, Niwa T, et al. Amphiphilic Polysaccharide Nanogels as Artificial Chaperones in Cell-Free Protein Synthesis [J]. *Macromol Biosci*, 2011, 11(6): 814-820.

57. Sekine Y, Moritani Y, Ikeda-Fukazawa T, et al. A Hybrid Hydrogel Biomaterial by Nanogel Engineering: Bottom-up Design with Nanogel and Liposome Building Blocks to Develop a Multidrug Delivery System [J]. *Adv Health Mater*, 2012, 1(6): 722-728.

58. Siegwart D J, Srinivasan A, Bencherif S A, et al. Cellular Uptake of Functional Nanogels Prepared by Inverse Miniemulsion Atrp with Encapsulated Proteins, Carbohydrates, and Gold Nanoparticles [J]. *Biomacromolecules*, 2009, 10(8): 2300-2309.